Circulation on the Continental Shelf of the Southeastern United States. Part I: Subtidal Response to Wind and Gulf Stream Forcing During Winter

THOMAS N. LEE, WEN JEI HO, VASSILIKI KOURAFALOU AND JOHN D. WANG

Rosenstiel School of Marine and Atmospheric Science, University of Miami, Miami, FL 33149

(Manuscript received 29 July 1983, in final form 19 March 1984)

ABSTRACT

Subtidal current and sea level response to wind and Gulf Stream forcing are investigated for the South Atlantic Bight shelf during winter conditions. Low-frequency flow variability in the outer shelf results primarily from wavelike meanders and eddies in the Gulf Stream front that occur in a 2-day to 2-week period band. Current meter derived vertically integrated momentum balances indicated that these large amplitude flow events are in approximate geostrophic balance with baroclinic pressure gradients induced by northward propagating Gulf Stream disturbances.

Low-frequency flow at midshelf is primarily a local Ekman response to wind forcing. Cross-shelf momentum balance for the total water column is between the along-shelf geostrophic current and the cross-shelf barotropic pressure gradient resulting from wind induced sea level changes at the coast. This balance holds for both mean and fluctuating parts of the flow, with the along-shelf barotropic current lagging sea level by 6 to 12 hours and along-shelf wind by 12 to 24 hours. The along-shelf balance of momentum is between the Coriolis force, along-shelf pressure gradient and along-shelf wind stress for the mean flow, with additional contribution from the local along-shelf acceleration of the water column and along-shelf bottom stress for the fluctuating flow. Near the transition from midshelf to outer-shelf flow regimes, which occurs at about the 40 m isobath, there is a significant contribution to mean and fluctuating along-shelf momentum from the divergence of cross-shelf transport of along-shelf momentum. An along-shelf slope of Gulf Stream origin of order -10^{-7} appears to make a significant contribution to the observed mean northward flow over the shelf. Mean volume transports are approximately 20×10^4 m^3 s^{-1} northward, which indicates a shelf residence time of three months.

1. Introduction

In Part I of this three part work we investigate the subtidal current and sea level response to wind and Gulf Stream forcing on the South Atlantic Bight (SAB) continental shelf during winter conditions. Data used in this study are from the GABEX-I experiment (Georgia Bight Experiment; Lee and Atkinson, 1983) and from the results of the numerical model discussed in the companion papers: (Wang *et al.*, 1984; Kourafalou *et al.*, 1984). This work is part of a Department of Energy and Minerals Management Service (formerly Bureau of Land Management) supported interdisciplinary study of the region.

Shelf topography in the study area is relatively simple, consisting of a broad, shallow, curved shelf that slopes gently to a rather sharp shelf break at about the 75 m isobath (Fig. 1). Maximum shelf widths of 120 km occur in the vicinity of Savannah, Georgia, and decrease to a minimum of 50 km off Cape Canaveral, Florida, the southern boundary of the domain. A shallow shoal extends east from Cape Fear and forms the northern boundary of the region. The shelf is bordered on the east by the strong northward flowing Gulf Stream. The western edge of the Gulf Stream tends to follow the shelf break between Cape Canaveral and Savannah (Bane and Brooks, 1979). Downstream of the topographic feature known as the Charleston Bump, the Gulf Stream front exhibits greater variability in its position and tends to be located farther east of the shelf break on the mean (Legeckis, 1979; Bane and Brooks, 1979; Olson *et al.*, 1983).

Low-frequency ($f < 0.6$ cpd) current and temperature variability in the outer shelf (depths > 40 m) has been shown to be dominated by northward propagating Gulf Stream meanders and eddy events in the period band of 2 days to 2 weeks with no apparent relation to wind forcing (Lee and Brooks, 1979; Lee *et al.*, 1981; Lee and Atkinson, 1983). Along the landward boundary a series of small to moderate size rivers discharge fresh water into the inner shelf region (0–20 m isobaths as defined by Atkinson *et al.*, 1983), which tends to form a nearshore band of stratified, less saline waters with a persistent southward baroclinic flow (Bumpus, 1973; Blanton, 1981). The midshelf zone (21–40 m isobaths) exhibits seasonal changes in stratification; with vertical homogeneous conditions prevailing during the fall and winter seasons of intensified wind mixing, and vertically stratified waters typifying spring and summer periods of increased runoff and decreased wind mixing (Atkinson *et al.*, 1983).

Low-frequency current variability in the midshelf

region during winter has been shown to be strongly dependent on local wind forcing in the 2-day to 2-week period band dominated by atmospheric cold fronts (Lee and Brooks, 1979; Klinck *et al.*, 1981; Lee and Atkinson, 1983). The current response appears to follow simple Ekman frictional equilibrium dynamics similar to that observed in the Mid-Atlantic Bight (Beardsley and Butman, 1974; Scott and Csanady, 1976; Beardsley and Winant, 1979), and on the west coast (Hickey and Hamilton, 1980; Hickey, 1981). No convincing evidence of the existence of southward propagating shelf waves has been observed in coastal sea level or current meter measurements in the SAB in contrast to the steeper west coast shelves (Pietrafesa and Janowitz, 1980; Lee and Atkinson, 1983).

2. Observational techniques and data analysis

As part of the GABEX-I experiment, an array of 25 subsurface current meter moorings was deployed on the SAB shelf for a 4.5 month period from 16 February to 2 July 1980 (Fig. 1). Moorings were placed along cross-shelf transects at the 15, 28, 40 and 75 m isobaths. The moorings on the 15 and 28 m isobaths were deployed by L. Pietrafesa of NCSU and those at 40 and 75 m by T. Lee of UM. A discussion of the array design and detailed analysis of data from the 40 and 75 m isobaths can be found in Lee and Atkinson (1983). Here we are more concerned with data from midshelf (28 and 40 m isobaths) and outer shelf (75 m isobath) along the 30°N transect. Moorings from

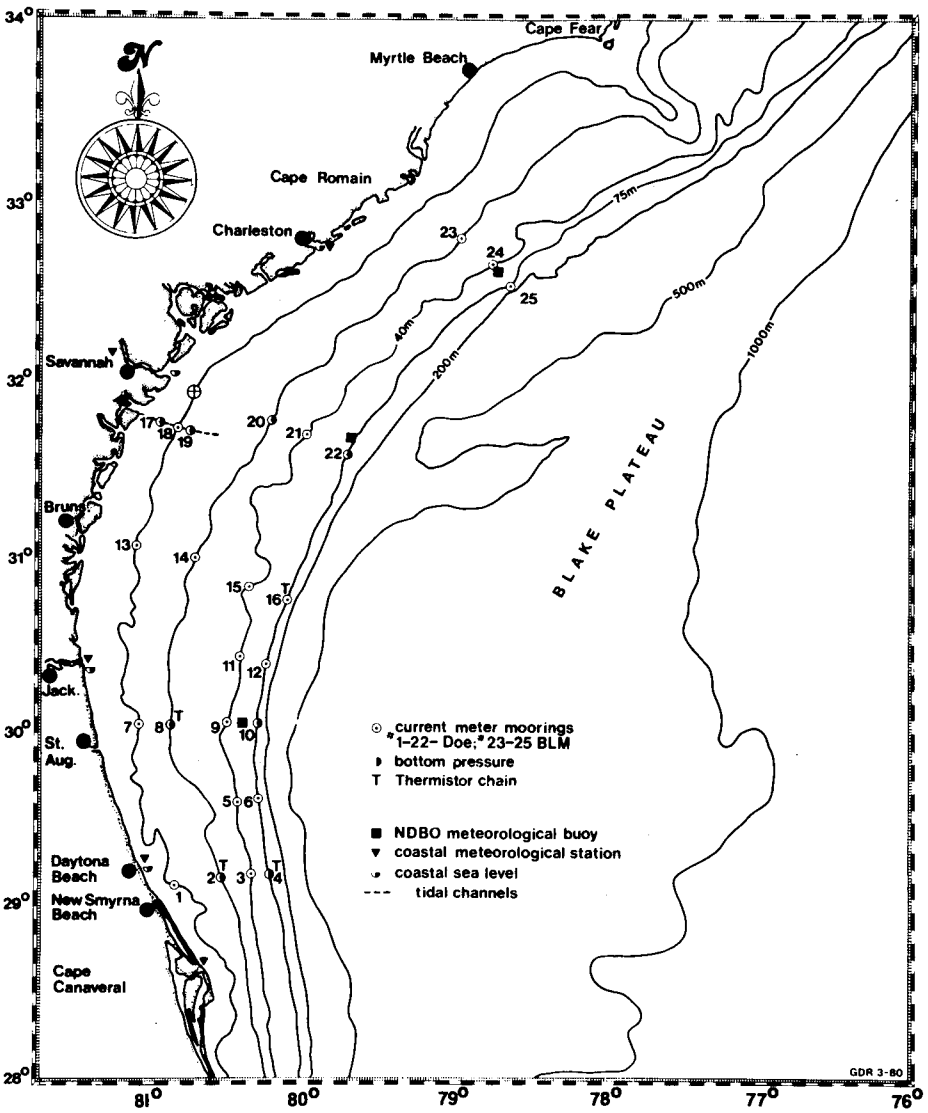

FIG. 1. GABEX-I subsurface current meter array, 17 February to 26 June 1980.

these locations were equipped with the greatest number of current meters and the data are typical of the other sites. Mooring 10 on the 75 m isobath was instrumented with 6 current meters at depths of 7, 17, 27, 37, 45, 60 and 72 m; mooring 9 on the 40 m isobath had current meters at 7, 17, 27 and 37 m; and mooring 8 on the 28 m isobath had current meters at 7, 17 and 25 m depths. Data from the 40 and 75 m sites were of good quality for the total 4.5 month experiment. At the 28 m site the upper current meter failed, and only one month of data was obtained from the 17 and 25 m depths. Current speed measurements at the 25 m depth had to be corrected for biofouling by comparison with the 17 m level speeds. Shelf wind data were obtained from NDBO buoy 41003 stationed between moorings 9 and 10 and from coastal stations as shown on Fig. 1. Coastal sea level data were obtained from the NOS Savannah River site, and bottom pressure data were recorded at mooring sites 1, 17 and 22. Atmospheric pressure was added to the coastal sea level data to form synthetic subsurface pressure (SSP) records. Subsequently the mean was subtracted from

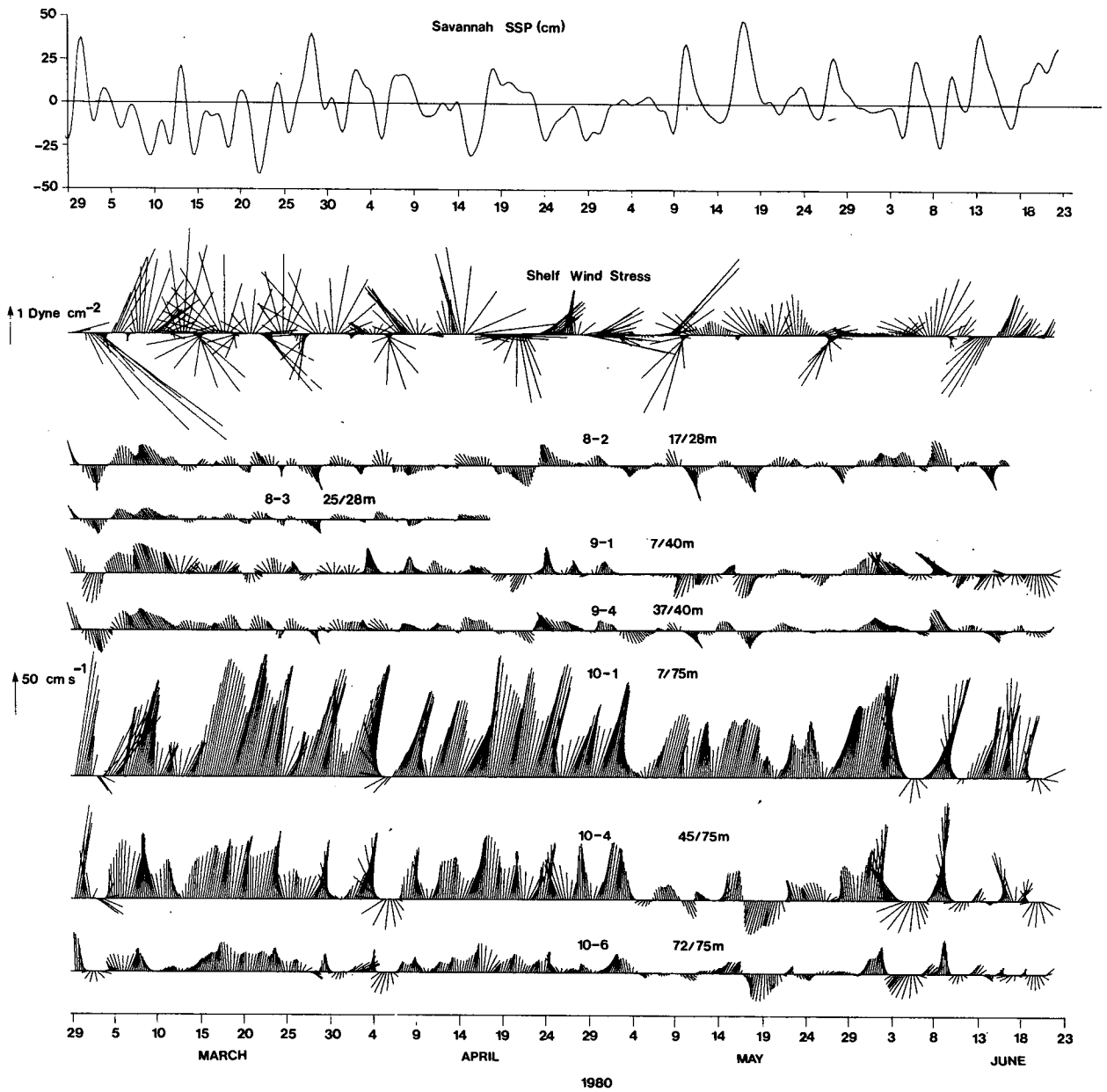

FIG. 2. Time series 6 h rotated, 40 HLP current vectors from moorings 8, 9 and 10 (at 30°N) of the GABEX-I array. Shelf wind stress and coastal SSP from the Savannah River site are also shown for the same time period.

all bottom pressure and coastal SSP records to form demeaned time series.

Low-frequency (subtidal) time series of all datasets were obtained by filtering with a 40 h low-pass Lanczos filter kernel to remove variance associated with tidal and inertial motions. Semidiurnal tides are attenuated by more than 10^5 by the filter, which results in a 4-day truncation at the start and end of the records. The filtered data were subsampled every 6 h, and current and wind vectors were rotated to align with the local topography, such that the velocity components (u, v) are positive in the offshore and northward along-shelf directions, respectively.

Wind velocities were converted to stress vectors by

$$\tau_s = \rho_{\text{air}} C_D |\mathbf{V}_{10}| \mathbf{V}_{10},$$

where ρ_{air} is the density of air; $\mathbf{V}_{10}$ is the wind vector measured approximately 10 m above the surface; C_D is the drag coefficient and is taken as a constant 1.5×10^{-3}.

Time series of vertical average velocities were derived for use in momentum calculations by making simple averages of the velocity components from each mooring. Hydrographic data collected by Skidaway Institute of Oceanography were used to compute the baroclinic pressure gradient terms, $(g/H\rho_0) \int_{-h}^{0} (\partial\alpha/\partial x) dz$ (discussed later), for midshelf where salinity variations can have a significant effect on denity. In the outer-shelf these terms could be estimated directly from the moored temperature time series using the near linear density–temperature relationships for Gulf Stream waters in this region.

3. Low-frequency fluctuations

Subtidal frequency current records are shown in Fig. 2 along with shelf wind stress and coastal SSP from the Savannah River site. The Gulf Stream influence is clearly indicated in the outer shelf records where current speeds reached 150 cm s^{-1} toward the north and mean speeds of 60 cm s^{-1} occurred in the upper layer. Vertical shears were on the order of 10^{-2} s^{-1} for the mean and fluctuating flows (Figs. 2 and 3) and were approximately balanced by horizontal density gradients, indicating a significant baroclinic component to both mean and fluctuating parts of the flow. Subtidal current variability at the outer shelf was found to be mainly produced by cold, cyclonic Gulf Stream frontal eddies propagating northward at a mean speed of 55 cm s^{-1} and mean period of 6 days, with no significant correlation with wind or coastal SSP events (Lee and Atkinson, 1983).

In contrast, current fluctuations at the 28 and 40 m isobaths are poorly correlated with events at the shelf break and show strong correlation with wind and coastal SSP. Spectral analysis showed along-shelf currents to be highly coherent with an along-shelf wind

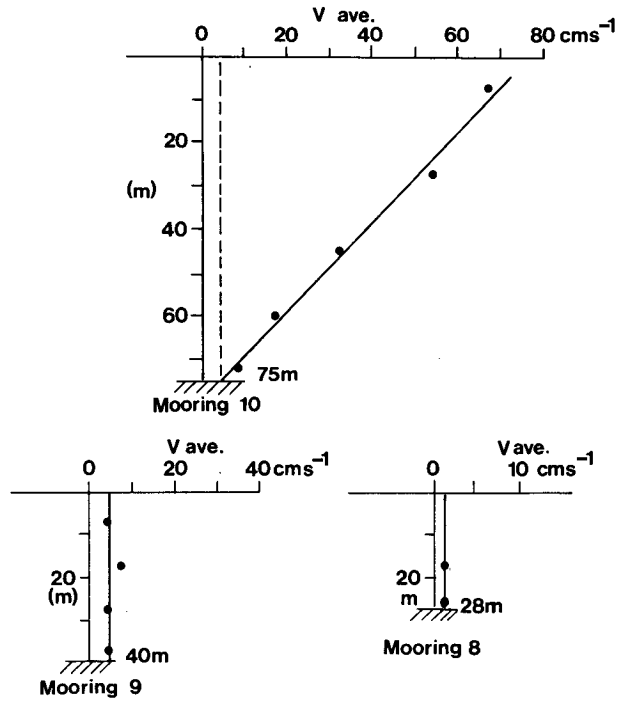

FIG. 3. Mean along-shelf current profiles from the 28, 40 and 75 m isobaths (moorings 8, 9 and 10 respectively). Solid dots give current meter derived averages. Straight lines are hand-fitted to the mean values.

and coastal SSP at periods of 3–4 and 10–12 days. Current fluctuations were nearly equal in magnitude and close in phase over instrument vertical separations at the 28 and 40 m isobaths (Fig. 2) and horizontal spacings greater than 400 km, indicating a local barotropic response to wind forcing (Lee and Atkinson, 1983). Along-shelf mean flows were also nearly uniform with depth at speeds of about 1 and 5 cm s^{-1} northward at 28 and 40 m, respectively (Fig. 3).

4. The Ekman frictional equilibrium response to wind forcing

Simple Ekman dynamics predicts that for a northward along-shelf wind an offshore transport will occur in the surface friction layer that will cause a set-down of coastal sea level, which in turn will maintain a northward geostrophic interior flow,

$$V_g = \frac{g}{f} \frac{\partial \eta}{\partial x},$$

where η is sea surface elevation (Beardsley and Butman, 1974; Lee and Brooks, 1979). The opposite occurs for southward winds. Scott and Csanady (1976) have shown that by sorting wind and near bottom current data from the Mid-Atlantic Bight into a different category defined by wind events and then averaging, a

frictional equilibrium resulted for the balance of along-shelf momentum of the entire water column:

$$\tilde{\tau}_{ys} = gh\frac{\partial \eta}{\partial y} + \tilde{\tau}_{yb}, \quad (1)$$

where $\tilde{\tau}_{ys}$ is the event averaged surface stress in the y direction, $\tilde{\tau}_{yb} = r\tilde{V}_b$, r is a bottom resistance coefficient and $\tilde{V}_b$ the event averaged near bottom velocity. Tebeau and Lee (1979) found a similar balance for midshelf flow measurements in the SAB during winter conditions. They reported a resistance coefficient of 0.1 cm s^{-1} whereas Scott and Csanady found 0.16 cm s^{-1}. Using a typical magnitude for bottom velocity events of 20 cm s^{-1} (Fig. 2) implies a drag coefficient of $C = 5 \times 10^{-3}$ for midshelf. Tebeau and Lee used Eq. (1) to estimate a mean along-shelf slope of $\partial\eta/\partial y = -1.67 \times 10^{-7}$, which is almost exactly what Sturges (1974) found for the region using geostrophic and steric leveling in the Gulf Stream.

Evidence supporting an Ekman response to local wind forcing is clearly indicated in current, coastal SSP and bottom pressure data (Fig. 4). The SSP and pressure data are demeaned time series. Vertically averaged along-shelf currents are shown for moorings 8, 9 and 10 together with shelf wind stress. Bottom pressure and coastal SSP fluctuations indicate high coherence between all stations with small phase lags. These fluctuations are also highly correlated with wind events in the 2–14 day period band, indicating that bottom pressure variations in the weather band are predominantly produced by changes in sea level rather than density (barotropic rather than baroclinic). Some exceptions to this may occur at times at the shelf break (Station 22). Low-frequency variations in cross and along-shelf sea level slopes (interpreted from bottom pressure differences) appear to result largely from amplitude differences between stations. Greatest amplitudes (±10 to 30 cm) occurred at the coast near Savannah, where the shelf is widest, and decreased offshore to ±7 to 20 cm at the 15 m isobath (stations 1 and 17) and ±3 to 7 cm at the shelf break (station 22).

Sea level slopes and barotropic flows at the 28 and 40 m isobaths appear to be a direct response to local wind forcing. Northward winds (event lines in Fig. 4) that are coherent over the shelf domain, cause a greater drop in sea level near the coast than at the shelf edge. This results in a positive cross-shelf slope that is highly coherent with and leads the northward barotropic flow. Lee and Atkinson (1983) determined from cross-spectral analysis that cross-shelf slopes led along-shelf flow events by 6–12 hours. The opposite occurs for southward winds. Along-shelf slopes were often 180° out of phase with cross-shelf slopes, which seems to be a consequence of greater sea level fluctuations near Savannah (events 1–11, Fig. 4). Amplitudes of the along-shelf sea level differences were approximately equal to the cross-shelf differences. Thus, a northward wind can also cause a negative along-shelf slope in the region south of Savannah that can further enhance the northward barotropic flow induced by a positive cross-shelf slope (Scott and Csanady, 1976). If sea level fluctuations are maximum in the Savannah area, then north of this region the along-shelf slope would be of opposite sign.

Figure 4 also indicates a very long period oscillation in along-shelf sea level slope that may be related to either wind or density effects. During March the mean winds were toward the northeast and the along-shelf slope was mostly negative at the 15 m isobath. Since sea level setdown would be greater at Savannah for these winds, a negative slope would result. However, in April and May the along-shelf slope was mostly positive. This occurred about the time of the spring increase in river runoff (Atkinson *et al.*, 1983) which would cause density to decrease in the vicinity of the Savannah River outflow and could cause sea level to stand higher off Savannah relative to New Smyrna Beach. The reciprocal of this trend is apparent in the cross-shelf sea level slope off Savannah as well and may also be an effect of the fresh water discharge collecting primarily in the nearshore zone (Atkinson *et al.*, 1983).

5. Vertically integrated momentum balances

To better understand and quantify the dynamic responses of the shelf waters to variable forcing events the array data were used to compute vertically integrated momentum balances. These equations can be written in conservation form for the cross-shelf (x) and along-shelf (y) vertical average velocity components ($\bar{u}$, $\bar{v}$) as

$$\frac{\partial \bar{u}}{\partial t} + \frac{\partial \bar{u}^2}{\partial x} + \frac{\partial \bar{u}\bar{v}}{\partial y} - f\bar{v} = -g\frac{\partial \eta}{\partial x} - \frac{g}{H\rho_0}\int_{-h}^{0}\frac{\partial \alpha}{\partial x}dz + \frac{\tau_{xs}}{\rho_0 H} - \frac{\tau_{xb}}{\rho_0 H}, \quad (2)$$

$$\frac{\partial \bar{v}}{\partial t} + \frac{\partial \bar{v}^2}{\partial y} + \frac{\partial \bar{u}\bar{v}}{\partial x} + f\bar{u} = -g\frac{\partial \eta}{\partial y} - \frac{g}{H\rho_0}\int_{-h}^{0}\frac{\partial \alpha}{\partial y}dz + \frac{\tau_{ys}}{\rho_0 H} - \frac{\tau_{yb}}{\rho_0 H}, \quad (3)$$

where horizontal friction has been neglected and

$$\bar{(\ )} = \frac{1}{H}\int_{-h}^{\eta}(\ )dz$$

$$H = \eta + h$$

$$\alpha = \int_{-z}^{0}\rho dz$$

ρ density, reference density $\rho_0 = 1.0$

z vertical coordinate positive upwards from mean sea level at $z = 0$

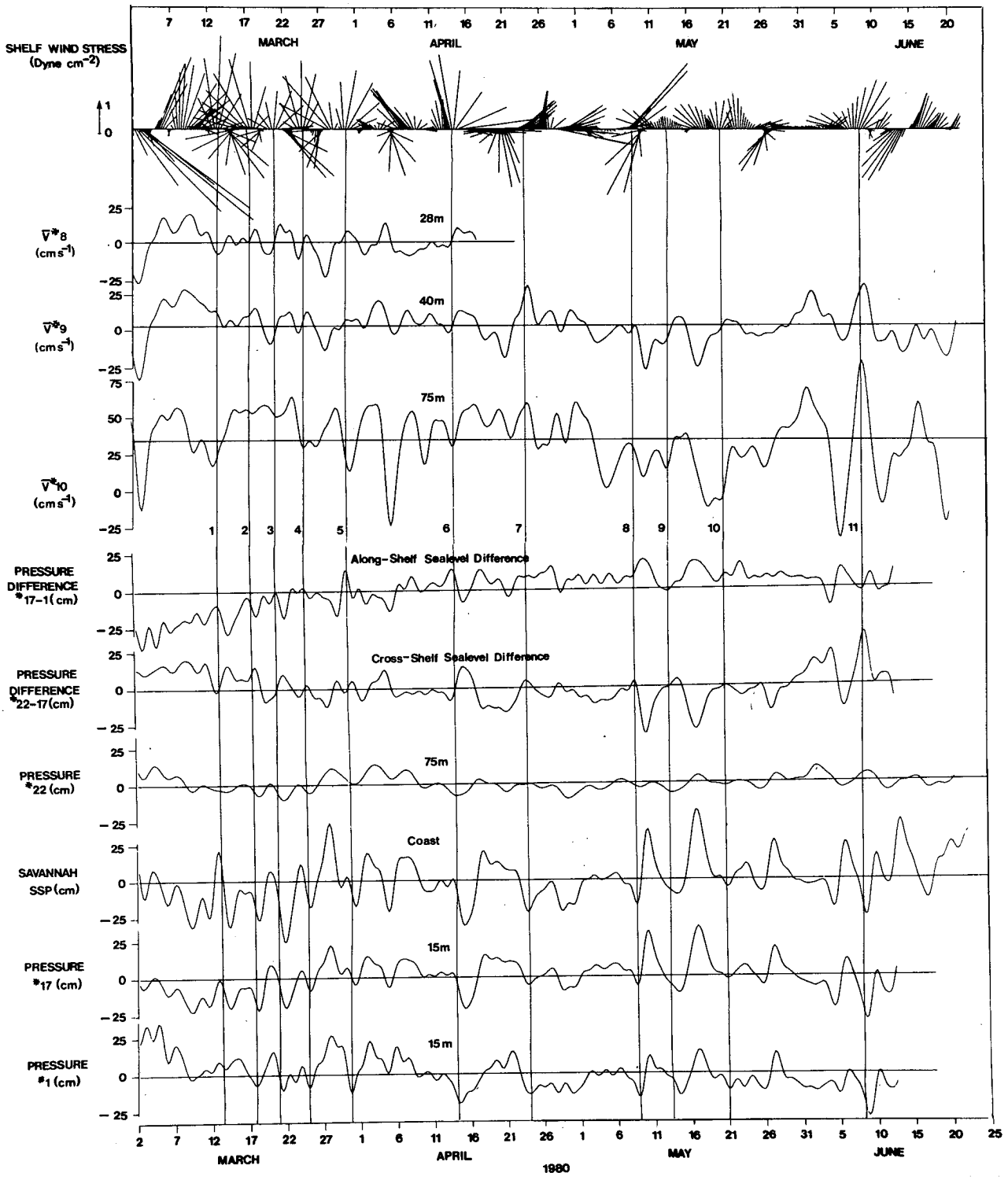

FIG. 4. Coastal synthetic subsurface pressure (SSP) from Savannah River, shelf wind stress and current vectors from the 75, 40 and 28 m isobaths at 30°N during GABEX-I. All data filtered with a 40 HLP filter and subsampled every 6 h. Instrument and water depths shown next to current meter identification.

TABLE 1. Term estimates of the vertically integrated momentum equations for the 28 m isobath from 40 HLP filtered data. The η time series are demeaned. The larger term estimates are underlined.

	Momentum term ($\times 10^{-4}$ cm s^{-2})							
	Cross-shelf							
	$\frac{\partial \bar{u}}{\partial t}$ +	$\frac{\partial \bar{u}^2}{\partial x}$ +	$\frac{\partial \bar{u}\bar{v}}{\partial y}$ −	$f\bar{v}$ =	$-g\frac{\partial \eta}{\partial x}$ −	$\frac{g}{H\rho_0}\int_{-h}^{0}\frac{\partial \alpha}{\partial x}dz$ +	$\frac{\tau_{xs}}{\rho_0 H}$ −	$\frac{\tau_{xb}}{\rho_0 H}$
Mean	−0.03	+0.05	+0.01	<u>−1.0</u> =	<u>−1.6</u>	+0.3	+0.3	+0.05
Standard deviation	±0.6	±0.2	±0.04	<u>±7.0</u> =	<u>±7.0</u>	(0.2–2.8)	<u>±2.5</u>	±0.3
	Along-shelf							
	$\frac{\partial \bar{v}}{\partial t}$ +	$\frac{\partial \bar{v}^2}{\partial y}$ +	$\frac{\partial \bar{u}\bar{v}}{\partial x}$ +	$f\bar{u}$ =	$-g\frac{\partial \eta}{\partial y}$ −	$\frac{g}{H\rho_0}\int_{-h}^{0}\frac{\partial \alpha}{\partial y}dz$ +	$\frac{\tau_{ys}}{\rho_0 H}$ −	$\frac{\tau_{yb}}{\rho_0 H}$
Mean	0.03	−0.001	−0.04	<u>−0.6</u> =	<u>−1.4</u>	—	<u>+0.8</u>	+0.03
Standard deviation	<u>±1.2</u>	±0.06	±0.2	<u>±2.7</u> =	<u>±3.6</u>	(0.1–1.9)	<u>±3.2</u>	<u>±0.6</u>

τ_{xs}, τ_{ys} surface wind stress components as given previously

$\tau_{xb} = C_{\rho 0}(u_b^2 + v_b^2)^{1/2}u_b$

$\tau_{yb} = C_{\rho 0}(u_b^2 + v_b^2)^{1/2}v_b$

u_b, v_b near bottom velocity components

$C = gn^2/H^{1/3}$

n Manning's coefficient (=0.025 m$^{-1/3}$ s).

First-order statistics of each of the terms in the momentum equations are given in Tables 1–3 for the 28, 40 and 75 m isobaths at the 30°N transect. Time series of the more important terms are shown in Figs. 5–8 for the midshelf and shelf break. The terms omitted are not significantly different from zero and do not affect the momentum balances. Cross- and along-shelf derivatives are computed with data from moorings 8, 9 and 20 (Fig. 1) for the 28 m isobath; moorings 9, 10 and 21 for the 40 m isobath, and 9, 10 and 22 for the 75 m isobath. Derivatives of η in x and y were determined from bottom pressure measurements at moorings 1, 17 and 22. Mean values of $\partial\eta/\partial x$ and $\partial\eta/\partial y$ could not be computed directly from the data due to depth uncertainties of the bottom pressure gauges. The mean slopes listed in the tables are the values necessary to balance the other terms. The baroclinic pressure terms

$$\frac{g}{H\rho_0}\int_{-h}^{0}\frac{\partial \alpha}{\partial x}dz,$$

at the 28 m isobath, were estimated from CTD stations. Due to lack of data, these values are not statistically meaningful, but since density changes at midshelf are relatively slow, compared to wind influenced changes in surface slope, the estimates may be characteristic of slowly varying conditions. No estimates of the baroclinic pressure terms were made for the 40 m isobath. At the 75 m isobath the baroclinic terms were estimated directly from temperature measured by the current meters.

TABLE 2. Term estimates of the vertically integrated momentum equations for the 40 m isobath from 40 HLP filtered data. The η time series are demeaned. The larger term estimates are underlined.

	Momentum terms ($\times 10^{-4}$ cm s^{-2})							
	Cross-shelf							
	$\frac{\partial \bar{u}}{\partial t}$ +	$\frac{\partial \bar{u}^2}{\partial x}$ +	$\frac{\partial \bar{u}\bar{v}}{\partial y}$ −	$f\bar{v}$ =	$-g\frac{\partial \eta}{\partial x}$ −	$\frac{g}{H\rho_0}\int_{-h}^{0}\frac{\partial \alpha}{\partial x}dz$ +	$\frac{\tau_{xs}}{\rho_0 H}$ −	$\frac{\tau_{xb}}{\rho_0 H}$
Mean	0.003	−0.7	+0.03	<u>−6.0</u> =	<u>−6.4</u>	—	+0.2	+0.2
Standard deviation	±0.6	±0.8	±0.06	<u>±8.6</u> =	<u>±7.4</u>	—	<u>±1.8</u>	±0.4
	Along-shelf							
	$\frac{\partial \bar{v}}{\partial t}$ +	$\frac{\partial \bar{v}^2}{\partial y}$ +	$-\frac{\partial \bar{u}\bar{v}}{\partial x}$ +	$-f\bar{u}$ =	$-g\frac{\partial \eta}{\partial y}$ −	$\frac{g}{H\rho_0}\int_{-h}^{0}\frac{\partial \alpha}{\partial y}dz$ +	$\frac{\tau_{ys}}{\rho_0 H}$ −	$\frac{\tau_{yb}}{\rho_0 H}$
Mean	0.1	−0.08	<u>+2.8</u>	<u>−1.7</u> =	<u>1.0</u>	—	<u>+0.5</u>	<u>−0.4</u>
Standard deviation	<u>±1.3</u>	±0.1	<u>±2.4</u>	<u>±3.0</u> =	<u>±3.6</u>	—	<u>±2.2</u>	<u>±1.0</u>

TABLE 3. Term estimates of the vertically integrated momentum equations for the 75 m isobath from 40 HLP filtered data. The η time series are demeaned. The larger term estimates are underlined.

	Momentum term ($\times 10^{-4}$ cm s^{-2})							
	Cross-shelf							
	$\frac{\partial \bar{u}}{\partial t}$ +	$\frac{\partial \bar{u}^2}{\partial x}$ +	$\frac{\partial \bar{u}\bar{v}}{\partial y}$ −	$f\bar{v}$ =	$-g\frac{\partial \eta}{\partial x}$ −	$\frac{g}{H\rho_0}\int_{-h}^{0}\frac{\partial \alpha}{\partial x}dz$ +	$\frac{\tau_{xs}}{\rho_0 H}$ −	$\frac{\tau_{xb}}{\rho_0 H}$
Mean	0.04	+0.7	−0.2	<u>−31</u>	= −3	<u>−28</u>	+0.1	−0.1
Standard deviation	±1	±1	±0.3	<u>±16</u>	= <u>±7</u>	<u>±11</u>	±1	±0.2
	Along-shelf							
	$\frac{\partial \bar{v}}{\partial t}$ +	$\frac{\partial \bar{v}^2}{\partial y}$ +	$\frac{\partial \bar{u}\bar{v}}{\partial x}$ +	$f\bar{u}$ =	$-g\frac{\partial \eta}{\partial y}$ −	$\frac{g}{H\rho_0}\int_{-h}^{0}\frac{\partial \alpha}{\partial y}dz$ +	$\frac{\tau_{ys}}{\rho_0 H}$ −	$\frac{\tau_{yb}}{\rho_0 H}$
Mean	0.09	<u>−1.3</u>	<u>+2.8</u>	<u>+4.8</u>	= <u>5.3</u>	<u>+1.2</u>	+0.3	<u>−0.5</u>
Standard deviation	<u>±2.8</u>	<u>±1.2</u>	<u>±2.4</u>	<u>±6.1</u>	= <u>±3.6</u>	<u>±4.5</u>	<u>±1.2</u>	<u>±0.6</u>

Table 1 and Fig. 5 indicate that at midshelf the cross-shelf momentum balance of the fluctuating flow is reasonably accounted for by

$$f\bar{v} = g\frac{\partial \eta}{\partial x} - \frac{\tau_{xs}}{\rho_0 H}.$$

The cross-shelf slope appears to have the largest effect on the geostrophic flow. Time series of the baroclinic pressure term are not known due to the poor correlation between temperature and density at midshelf, but it is doubtful that this term would substantially improve the fit. The mean cross-shelf slope term is estimated from Table 1 to be O(1×10^{-4}), which is equivalent to the geostrophic term and is at least three times larger than the other terms. Therefore, in the mean the primary cross-shelf momentum balance appears to be geostrophic:

$$f\bar{v} \doteq g\frac{\partial \eta}{\partial x}.$$

In the along-shelf direction the balance between fluctuating components of momentum at midshelf is not as clear (Fig. 6), however the governing equation appears to be

$$\frac{\partial \bar{v}}{\partial t} + f\bar{u} = -g\frac{\partial \eta}{\partial y} + \frac{\tau_{ys}}{\rho_0 H} - \frac{\tau_{yb}}{\rho_0 H}.$$

Table 1 indicates that momentum changes within the water column, due to variations in the along-shelf slope, are about one-half as large as that produced by fluctuations in the cross-shelf slope. Density changes in the along-shelf direction are normally small, but large values can occur on occasion. For mean conditions the balance is

$$f\bar{u} = -g\frac{\partial \eta}{\partial y} + \frac{\tau_{ys}}{\rho_0 H},$$

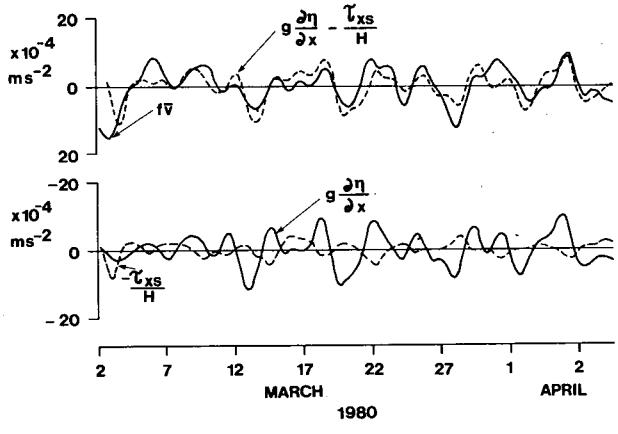

FIG. 5. Vertically averaged cross-shelf momentum balance 28 m isobath: derived from moorings 8, 9 and 20.

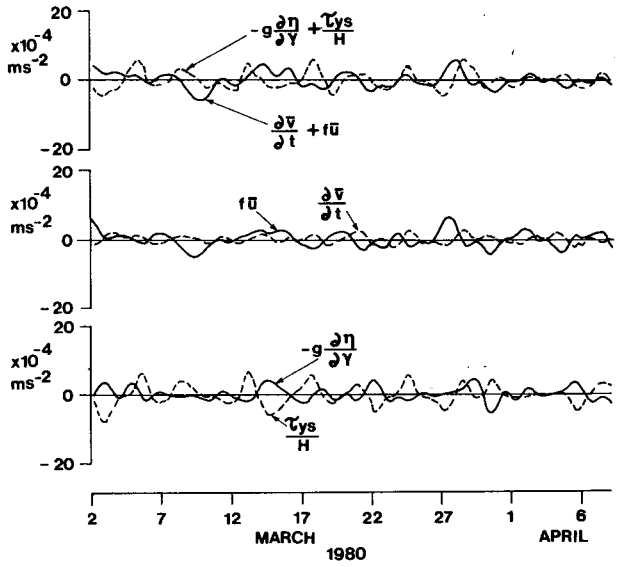

FIG. 6. As in Fig. 5 but for along-shelf.

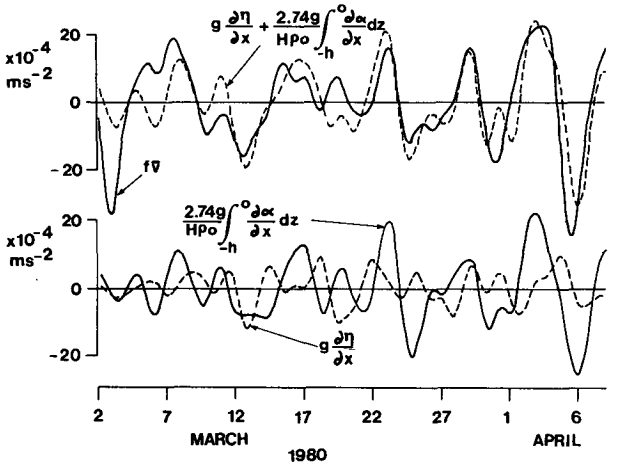

FIG. 7. As in Fig. 5 but at 75 m isobath; derived from moorings 9, 10 and 22.

where $\partial\eta/\partial y \approx O(1 \times 10^{-7})$ as determined from the other terms.

The cross-shelf momentum balances at the 40 m isobath are essentially the same as that found for midshelf for both the mean and fluctuating parts of the flow (Table 2). Along-shelf momentum balances are also the same as those found for midshelf except that the nonlinear momentum advection term $\partial\bar{u}\bar{v}/\partial x$ becomes important for the mean and fluctuation balances. This term was computed from data taken at the 40 and 75 m isobaths and so is not truly representative of the 40 m isobath but some midway location at about the 60 m isobath.

A mean along-shelf slope of order -10^{-7} is needed to balance mean along-shelf momentum at 40 m. This slope is close to previous estimates by Sturges (1974) who found -1.6×10^{-7} from geostrophic leveling in the Gulf Stream and -1.67×10^{-7} found by Tebeau and Lee (1979).

The mean advection of water column momentum, $\langle \partial\bar{u}\bar{v}/\partial x \rangle$, at 40 m is large and positive, which indicates that there was a net offshore advection of northward momentum. Lee and Atkinson (1983) have shown that the northward passage of Gulf Stream frontal eddies produces a net offshore flux of northward momentum $(+\langle u'v' \rangle)$ at this location, which transfers kinetic energy from the perturbations back to the mean flow of the Gulf Stream. Thus, the outer-shelf strip between 40 and 75 m water depths at 30°N appears to be a region where the Gulf Stream imparts mean northward momentum to the shelf through a net onshore flow and a negative along-shelf surface slope [due to the negative sign preceding this term in Eq. (3) and Table 2]. This momentum is locally compensated by an offshore advection of northward momentum arising from the passage of Gulf Stream frontal eddies.

Figure 7 indicates that at the shelf break the primary balance of cross-shelf fluctuating momentum is

$$f\bar{v} = g\frac{\partial\eta}{\partial x} + \frac{g}{H\rho_0}\int_{-h}^{0}\frac{\partial\alpha}{\partial x}\,dz$$

with the baroclinic pressure term apparently accounting for a larger fraction of the variance in geostrophic current judging from the similarity of the curves. However, $\int_{-h}^{0}(\partial\alpha/\partial x)dz$ is difficult to estimate in the outer shelf. Due to the steep bottom slope this term could only be estimated for the upper 40 m, which is the common depth for both mooring 9 and 10. This results in an underestimate of the term and requires an adjustment by an arbitrary factor of 2.74 to make the amplitudes of the fluctuating part of the baroclinic term approximately equal to that of the Coriolis term (as shown in Fig. 7). Fig. 3 shows a near linear decrease in mean along-shelf flow with depth from 67 cm s^{-1} at 7 m to 4 cm s^{-1} near bottom. This suggests that the mean flow is mostly baroclinic and that the near bottom flow results from the cross-shelf slope, which acts on the total water column and could produce the offset observed at the bottom. With this in mind we speculate that the near-bottom flow, which is 10% of the vertical average velocity, results from the barotropic pressure gradient component, leaving 90% of the vertical average flow for the baroclinic component. Thus, the contribution of the baroclinic term to the total cross-shelf momentum balance is estimated at 90% of the Coriolis term ($0.9 \times f\bar{v}$, see Table 3). The mean balance of cross-shelf momentum is approximated by

$$f\bar{v} = \frac{g}{H\rho_0}\int_{-h}^{0}\frac{\partial\alpha}{\partial x}\,dz.$$

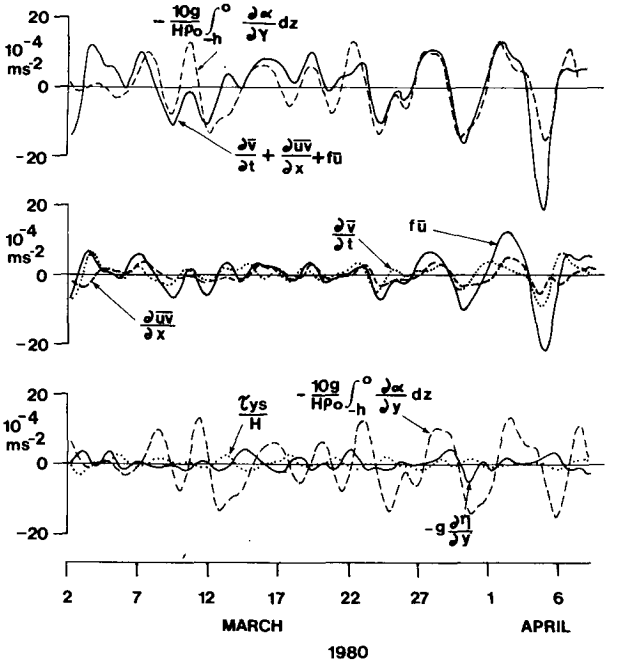

FIG. 8. As in Fig. 7 but for along-shelf.

In the along-shelf direction all the fluctuating terms are order one or greater at the shelf break except those evaluated in the surface layer (Table 3 and Fig. 8). Time series data suggest that the combination of local acceleration, nonlinear advection and the Coriolis term is significantly correlated with the along-shelf baroclinic pressure gradient advanced in time by 18 h. This indicates that the along-shelf baroclinic pressure gradient, associated with Gulf Stream frontal eddies, forces a cross-shelf geostrophic flow and significantly influences local acceleration of along-shelf momentum and cross-shelf momentum advection. However, the baroclinic term is not absolute and the magnitude had to be increased by a factor of 10 to be comparable to the Coriolis term in Fig. 8. The mean along-shelf momentum balance is also complicated at the shelf break, consisting mainly of

$$\frac{\partial \bar{v}^2}{\partial y} + \frac{\partial \overline{uv}}{\partial x} + f\bar{u} = -g\frac{\partial \eta}{\partial y} - \frac{g}{H\rho_0}\int_{-h}^{0}\frac{\partial \alpha}{\partial y}\,dz - \frac{\tau_{yb}}{\rho_0 H}$$

from which the along-shelf slope is estimated at $\partial\eta/\partial y = -5.3 \times 10^{-7}$ or about five times larger than found previously for the 40 m isobath.

6. Volume transports

Along-shelf volume transports were computed for the 30°N section using current meter data from moorings 8 and 9 (Fig. 9). Transports in the vicinity of each mooring were computed separately by multiplying the vertical average current by the cross-sectional area between: the 15 and 34 m isobaths for mooring 8 [$T_y(8)$]; and the 34 and 70 m isobaths for mooring 9 [$T_y(9)$]. These transports were then summed to produce the shelf transport between the 15 and 70 m isobaths. Outer shelf transports are not shown for they are strongly influenced by the Gulf Stream, which has large horizontal current shears, making it difficult to derive accurate transports from current meters.

Along-shelf volume transport ranged from ±85 $\times 10^4$ m^3 s^{-1} during an intense wind event near the start of the records. Typical transport fluctuations in the 2–14 day period band had amplitudes of 30–40 ($\times 10^4$ m^3 s^{-1}), and are highly coherent with wind events through the Ekman frictional response mechanism discussed earlier. Mean transport was northward at 16 $\times 10^4$ m^3 s^{-1} for the 41 day period. If the inner shelf waters between 0 and 15 m depths were included in this estimate, using the same northward mean current from site 8 of 1.4 cm s^{-1}, then the total mean along-shelf transport would be increased by only 0.2 $\times 10^4$ m^3 s^{-1}. Therefore, the volume transports calculated from data of moorings 8 and 9 should be reasonably good estimates of the total along-shelf transport.

In Kourafalou *et al.* (1984), we use a vertically integrated model to estimate an along-shelf volume transport of about 20 $\times 10^4$ m^3 s^{-1} toward the north due to an along-shelf slope of -1.67×10^{-7}. This transport is very close to that derived from current meter observations and suggests that the along-shelf slope is an important mechanism for driving the observed northward mean flow.

Mean along-shelf volume transports can be used to estimate shelf residence time, provided the 41-day av-

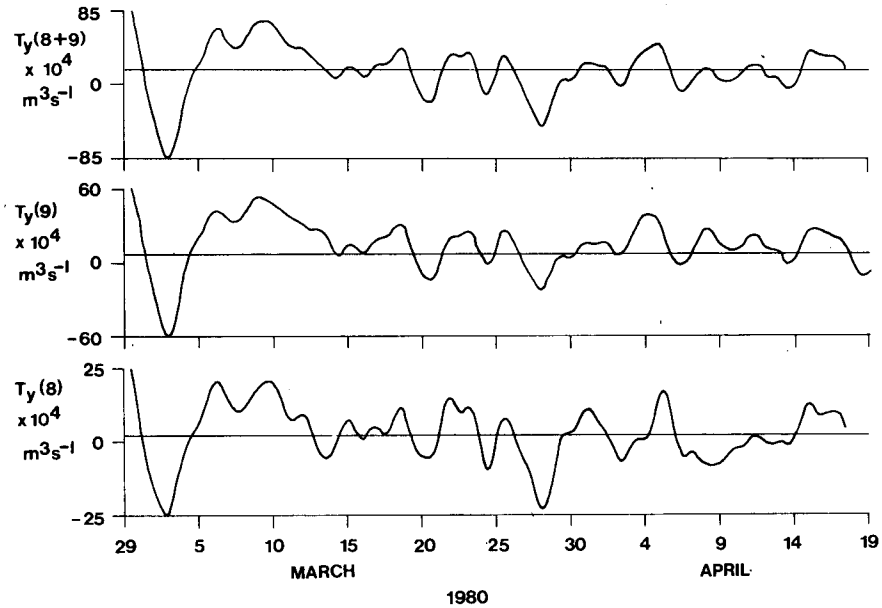

FIG. 9. Along-shelf volume transport (m^3 s^{-1}) between 15 and 34 m isobaths [$T_y(8)$]; 34 and 70 m isobaths [$T_y(9)$]; and 15 and 70 m isobaths [$T_y(8 + 9)$] computed from 40 HLP subtidal current records of GABEX-I.

erage is typical of long-term mean conditions. The volume of shelf water between Cape Canaveral and Cape Fear out to the 60 m isobath was estimated by Atkinson *et al.* (1983) at 1540 km^3. If the mean along-shelf transport is relatively constant over this region then it would take approximately three months to transport a volume equivalent to the shelf volume through the domain. Interestingly, previous estimates using salt conservation have also predicted shelf residence times of about 3 months (Atkinson *et al.*, 1978; Atkinson *et al.*, 1983).

7. Conclusions

Analysis of low-frequency currents on the SAB shelf during winter conditions lends further support to the concept of separation of flow regimes by the processes controlling variability (Lee and Brooks, 1979; Chao and Pietrafesa, 1980; Lee, Atkinson and Legeckis, 1981; Atkinson *et al.*, 1983; Lee and Atkinson, 1983). Estimates of vertically integrated momentum balances are useful for identifying important processes in each flow regime.

Low-frequency variability in the outer shelf (depths > 40 m) is dominated by northward propagating baroclinic events of Gulf Stream origin (meanders and eddies: Lee and Atkinson, 1983). Both the mean and fluctuating parts of the along-shelf flow appear to be in approximate geostrophic balance with the cross-shelf baroclinic pressure gradient. Along-shelf momentum balances are complicated in the outer shelf for all the terms in the momentum equation are of near equal magnitude for both the mean and fluctuations. However, the derived time series indicate that along-shelf fluctuations in the baroclinic pressure gradient from Gulf Stream frontal eddies is the driving force for the cross-shelf geostrophic flow, and also influences local acceleration of along-shelf momentum and cross-shelf momentum advection.

Low-frequency variability in the midshelf of the SAB during winter appears to follow simple, locally forced Ekman dynamics. Along-shelf winds, that are coherent over the shelf domain, generate offshore/onshore transports in the surface Ekman layer that cause sea level to rise or fall at the coast, and thus produce cross-shelf slopes that are in approximate geostrophic balance with an along-shelf barotropic interior flow. Sea level response to along-shelf wind forcing is greatest near the coast in the vicinity of Savannah, where the shelf is widest. This effect produces cross and along-shelf slopes in the 2–14 day period "weather band" that lag the wind events by 6–12 h (Lee and Atkinson, 1983). Along-shelf currents, with near zero phase lags over downstream coherent length scales greater than 400 km, lag the cross-shelf slopes by 6–12 h (Lee and Atkinson, 1983). There is little indication in this region of southward propagating continental shelf waves (Pietrafesa and Janowitz, 1980; Lee and Atkinson, 1983).

Vertically integrated momentum balances give further support for an Ekman response to local wind forcing. Cross-shelf momentum balances at both the 28 and 40 m isobaths indicate that the mean along-shelf flow is in geostrophic balance with the cross-shelf barotropic pressure gradient. The fluctuating flow has an additional contribution from the cross-shelf wind. The momentum balance in the along-shelf direction is between the Coriolis force, along-shelf sea level slope and along-shelf wind stress at midshelf for mean conditions, with an additional contribution from the local acceleration for the fluctuating part. At the 40 m isobath, which is close to the transition point between mid- and outer shelves, the mean along-shelf momentum balance is between the divergence of cross-shelf transport of along-shelf momentum, Coriolis force, along-shelf slope and along-shelf surface and bottom stresses. An along-shelf slope of order -10^{-7} is needed to balance the mean along-shelf momentum. This slope appears to be an important contributor to the observed mean northward flow over the shelf. Sturges (1974) found a similar slope in the Gulf Stream adjacent to the SAB shelf from both steric and geostrophic leveling, indicating a Gulf Stream origin for the slope. An along-shelf slope from oceanic sources was also reported by Csanady (1978) and Beardsley and Winant (1979) for the Mid-Atlantic Bight and is believed to be the force which drives the observed mean southwest flow over that shelf.

Apparently the Gulf Stream imparts northward momentum to the SAB shelf through the along-shelf surface slope and a net onshore flow in the southern part of the Bight, possibly in the vicinity of Cape Canaveral where the shelf begins to widen. The momentum gained is partially released locally at 30°N by an offshore momentum advection in Gulf Stream frontal eddies and over the shelf length by a net offshore transport in the vicinity of the Charleston bump (Lee and Atkinson, 1983).

The mean along-shelf volume transport on the SAB shelf during winter was northward at approximately 20×10^4 m^3 s^{-1}. This transport appears to result mostly from the mean along-shelf slope at the outer shelf as determined from observations and model results (Kourafalou *et al.*, 1984). Wang *et al.* (1984) also showed that the residual tidal current could make a significant contribution to the northward mean transport. The shelf residence time estimated from along-shelf transport is 3 months.

Acknowledgments. We thank J. Green and G. Rosiello for their technical assistance. Funding for this study was provided by the Department of Energy under Contract DE-AS05-76EV05163 and the Minerals Management Service (formerly Bureau of Land Management) Prime Contract AAT851-CT1-25 to Science Applications, Inc., of Raleigh, NC, Subcontract 11-82029-11. Special appreciation is extended to Dr.

L. J. Pietrafesa of North Carolina State University for providing current meter data from the 28 m isobath and bottom pressure data from the 15 m isobath. Funding for this data was provided by Department of Energy Contract DOE-AS09-74-00902.

REFERENCES

Atkinson, L., J. O. Blanton and E. Haines, 1978: Shelf flushing rates based on the distribution of salinity and fresh water in the Georgia Bight. *Coastal and Estuarine Mar. Sci.*, **7**, 464–472.

——, T. N. Lee, J. Blanton and W. S. Chandler, 1983: Climatology of the southeastern U.S. continental shelf waters. *J. Geophys. Res.*, **88**, 4705–4718.

Bane, J. M., Jr., and D. A. Brooks, 1979: Gulf Stream meanders along the continental margin from the Florida Straits to Cape Hatteras. *Geophys. Res. Lett.*, **6**, 280–282.

Beardsley, R. C., and B. Butman, 1974: Circulation on the New England continental shelf: Response to strong winter storms. *Geophys. Res. Lett.*, **1**, 181–184.

——, and C. D. Winant, 1979: On the mean circulation in the Mid-Atlantic Bight. *J. Phys. Oceanogr.*, **9**, 612–619.

Blanton, J. O., 1981: Ocean currents along a nearshore frontal zone on the continental shelf of the southeastern United States. *J. Phys. Oceanogr.*, **11**, 1627–1637.

Bumpus, D. G., 1973: A description of the circulation on the continental shelf of the east coast of the United States. *Progress in Oceanography*, Vol. 6, Pergamon, 111–156.

Chao, S., and L. J. Pietrafesa, 1980: The subtidal response of sea level to atmospheric forcing in the Carolina Capes. *J. Phys. Oceanogr.*, **10**, 1246–1255.

Csanady, G. T., 1978: The arrested topographic wave. *J. Phys. Oceanogr.*, **8**, 47–62.

Hickey, B. M., 1981: Alongshore coherence on the Pacific northwest continental shelf (January–April, 1975). *J. Phys. Oceanogr.*, **11**, 822–835.

——, and P. Hamilton, 1980: A spin-up model as a diagnostic tool for interpretation of current and density measurements on the continental shelf of the Pacific northwest. *J. Phys. Oceanogr.*, **10**, 12–24.

Klinck, J. M., L. J. Pietrafesa and G. S. Janowitz, 1981: Continental shelf circulation induced by a moving, localized wind stress. *J. Phys. Oceanogr.*, **11**, 836–848.

Kourafalou, V., J. D. Wang and T. N. Lee, 1984: Circulation on the continental shelf of the southeastern United States. Part III: Modeling the winter wind-driven flow. *J. Phys. Oceanogr.*, **14**, 1022–1031.

Lee, T. N., and D. Brooks, 1979: Initial observations of current, temperature and coastal sea level response to atmospheric and Gulf Stream forcing. *Geophys. Res. Lett.*, **6**, 321–324.

——, and L. P. Atkinson, 1983: Low-frequency current and temperature variability from Gulf Stream frontal eddies and atmospheric forcing along the southeast U.S. outer continental shelf. *J. Geophys. Res.*, **88**, 4541–4568.

——, —— and R. Legeckis, 1981: Observations of a Gulf Stream frontal eddy on the Georgia continental shelf, April 1977. *Deep-Sea Res.*, **28A**, 347–378.

Legeckis, R., 1979: Satellite observations of the influence of bottom topography on the seaward deflection of the Gulf Stream off Charleston, South Carolina. *J. Phys. Oceanogr.*, **9**, 483–497.

Olson, D. B., O. B. Brown and S. R. Emmerson, 1983: Gulf Stream frontal statistics from Florida Straits to Cape Hatteras derived from satellite and historical data. *J. Geophys. Res.*, **88**, 4569–4578.

Pietrafesa, L. J., and G. S. Janowitz, 1980: Lack of evidence of southerly propagating continental shelf waves in Onslow Bay, NC. *Geophys. Res. Lett.*, **7**, 113–116.

Scott, J. T., and G. T. Csanady, 1976: Nearshore currents off Long Island. *J. Geophys. Res.*, **81**, 5401–5409.

Sturges, W., 1974: Sea level slope along continental boundaries. *J. Geophys. Res.*, **79**, 825–830.

Tebeau, P. A., and T. N. Lee, 1979: Wind induced circulation on the Georgia shelf. Rep. No. 79003, University of Miami, 177 pp.

Wang, J. D., V. Kourafalou and T. N. Lee, 1984: Circulation on the continental shelf of the southeastern United States. Part II: Model development and application to tidal flow. *J. Phys. Oceanogr.*, **14**, 1013–1021.